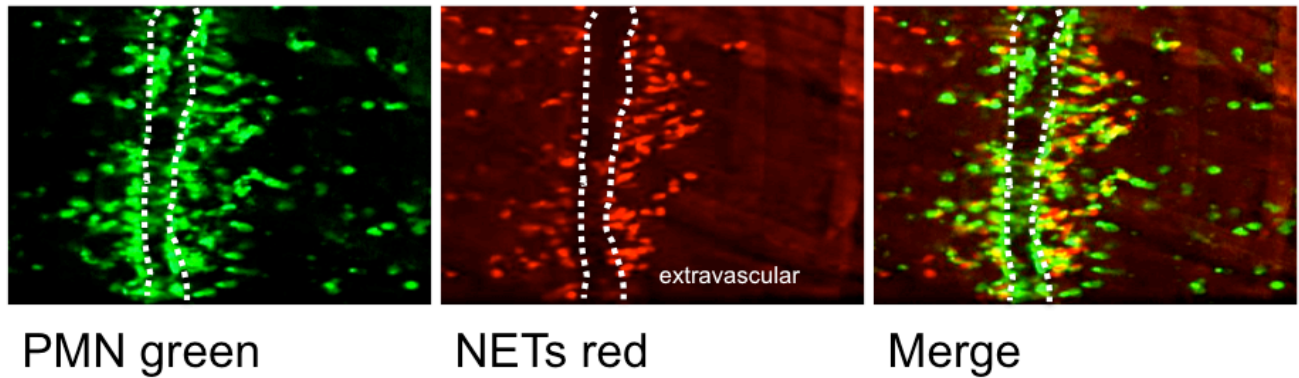


**Dynamic NETosis is Carried Out by Live Neutrophils in Human and Mouse Bacterial Abscesses and During Severe Gram-Positive Infection**

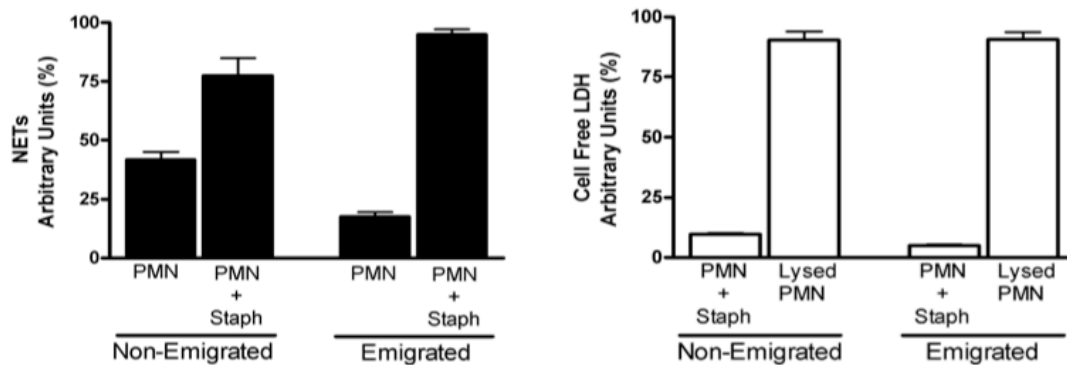
Bryan G. Yipp<sup>1,2,9</sup>, Björn Petri<sup>2,3,9</sup>, Davide Salina<sup>4</sup>, Craig N. Jenne<sup>1,2</sup>, Brittney N. V. Scott<sup>1,2,5</sup>, Lori D. Zbytnuik<sup>2,5</sup>, Keir Pittman<sup>2,5</sup>, Muhammad Asaduzzaman<sup>5</sup>, Kaiyu Wu<sup>3,4</sup>, H. Christopher Meijndert<sup>2</sup>, Stephen E. Malawista<sup>7</sup>, Anne de Boisfleury Chevance<sup>8</sup>, Kunyan Zhang<sup>2,3,4,6</sup>, John Conly<sup>2,3,4,6</sup> and Paul Kubes<sup>1,2,4,6</sup>

## Supplementary Figure 1

a



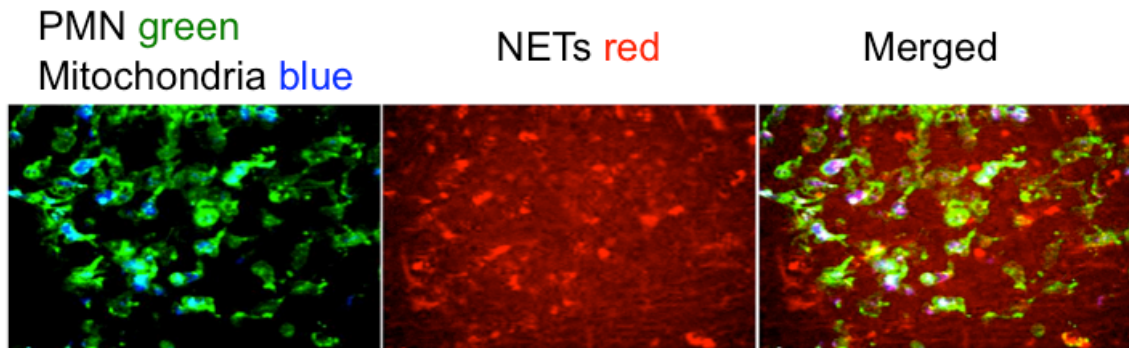
b



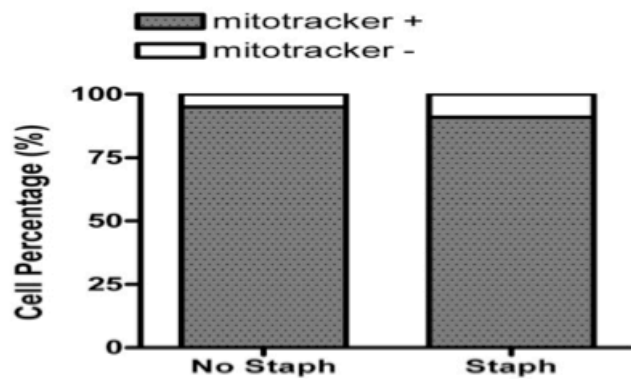
**Supplementary Figure 1.** Formation of NETs occurs in multiple tissues and is accentuated in emigrated neutrophils. Spinning disk confocal intravital microscopy was performed on the cremaster muscle of a mouse stimulated with MIP-2 superfusion (5 nM) and live *S. aureus* (Xen29,  $1 \times 10^8$  CFU in 100 $\mu$ l saline injection) was then directly injected into the muscle. PMN were labeled with GR-1 specific antibody and SYTOX Orange was used to visualize extracellular DNA. (a) PMN emigrating out of the microvessel, and the majority of extracellular DNA is outside of the vasculature and within the tissue ( $n = 4$ ). (b) NET formation in PMN either stimulated to emigrate into the mouse peritoneum or non-emigrated (bone marrow derived). Extracellular DNA was quantified using SYTOX Orange. Extracellular LDH from emigrated and non-emigrated PMN is shown on the right. Both emigrated PMN and non-emigrated PMN studies were performed 5 independent times (10 mice).

## Supplementary Figure 2

a

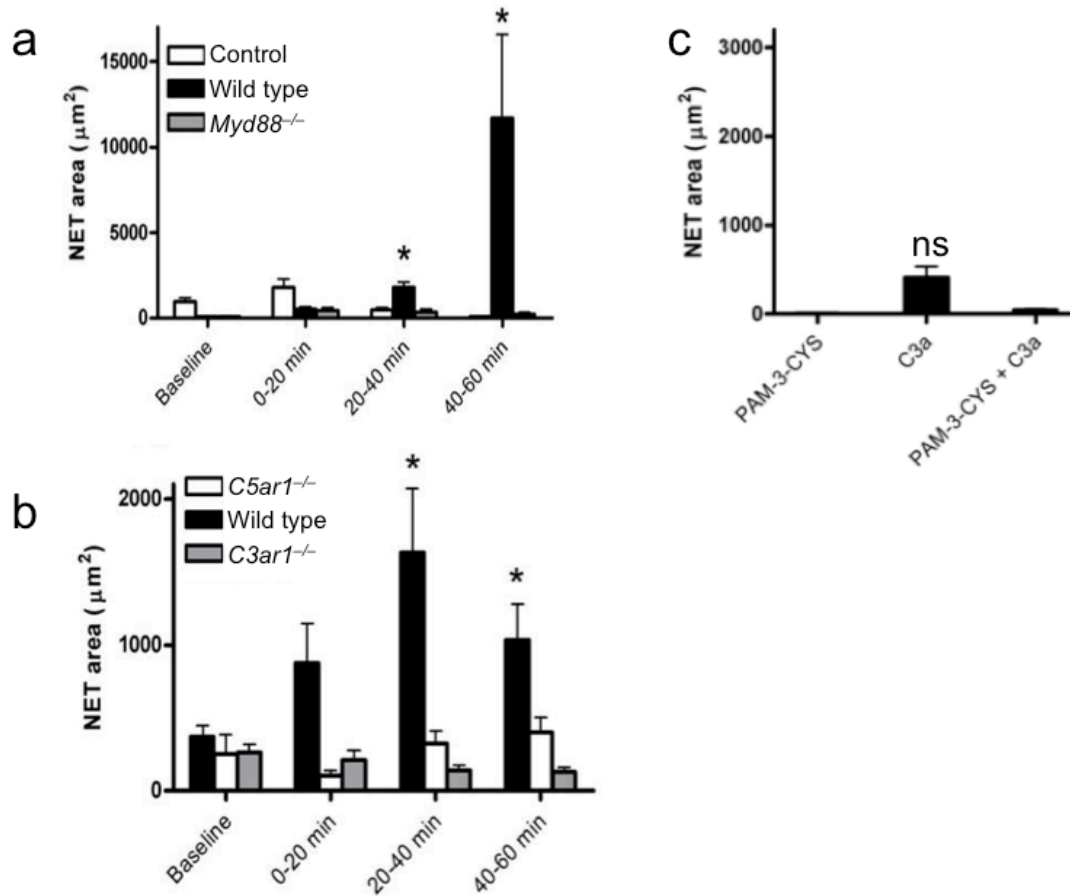


b



**Supplementary Figure 2.** The majority of NETs are derived from the nucleus during *in vivo* infection. Intact mitochondria were imaged *in vivo* with the addition of MitoTracker (1  $\mu$ l of 1 mM stock injected intravenously in sterile saline) and PMN with visible mitochondria were quantified. **(a)** Representative *in vivo* images demonstrating neutrophils with intact mitochondria making histone positive NETs post-staphylococcus. Merge of neutrophils and MitoTracker (left image), Extracellular histone (red)(middle image), and merge of neutrophils, MitoTracker and NETs (right image)( $n = 4$  mice). **(b)** Data represent the percentage of mitochondria positive neutrophils observed during 60 min ( $n = 6$  mice).

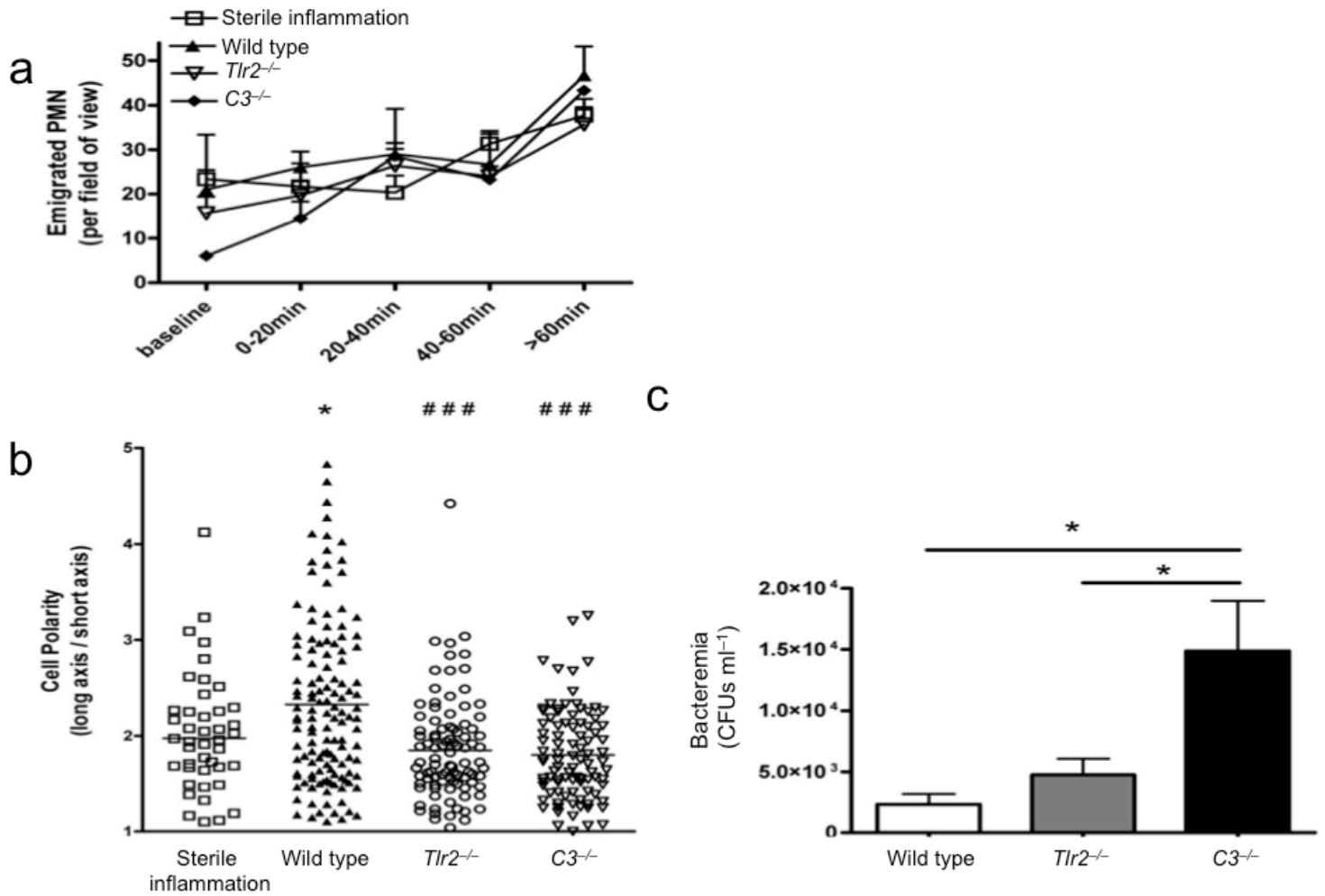
### Supplementary Figure 3



**Supplementary Figure 3.** *In vivo* NET formation requires Myd88 and Complement Receptors. Spinning disk confocal intravital microscopy was performed on the mouse skin model. MIP-2 (0.2 µg intradermal) was administered followed by a local injection of live *S. aureus* (Xen8.1,  $1 \times 10^8$  CFU per 100 µl saline injection). (a) NETs were visualized using a Xenon Alexa-549 labeled histone specific antibody. Wild type animals (C57Bl/6) had significant increases in NET area at 20 min compared to either *Myd88*<sup>-/-</sup> or the labeled IgG control (\* =  $P < 0.05$ ) (Three independent experiments were performed for each group with a total of nine mice). (b) Mice deficient in either the C5a or the C3a receptor were compared to appropriate wild type controls. NETs were visualized using the histone specific antibody. In wild type mice treated with live *S. aureus* NET area increased at 20 min and was statistically different from either mutant (Three independent experiments were performed for each group with 9 mice. \* =  $P < 0.05$ ) (c) Recombinant C3a (250 ng intradermal), purified PAM-3-CYS (5

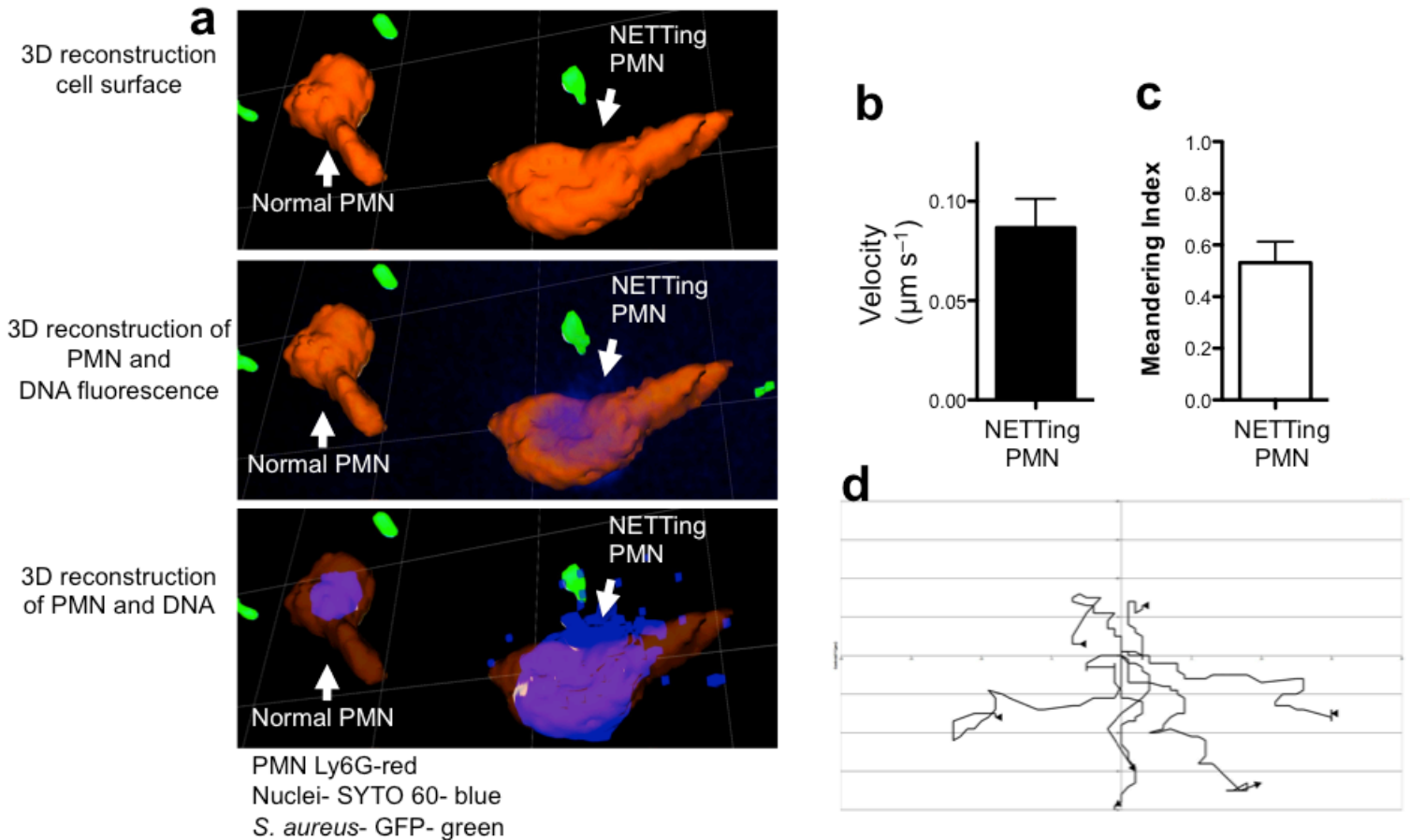
$\mu\text{g}$  intradermal) or both was used in place of live staphylococcus and NET area determined after 60 min (3 mice were used for each group).

## Supplementary Figure 4



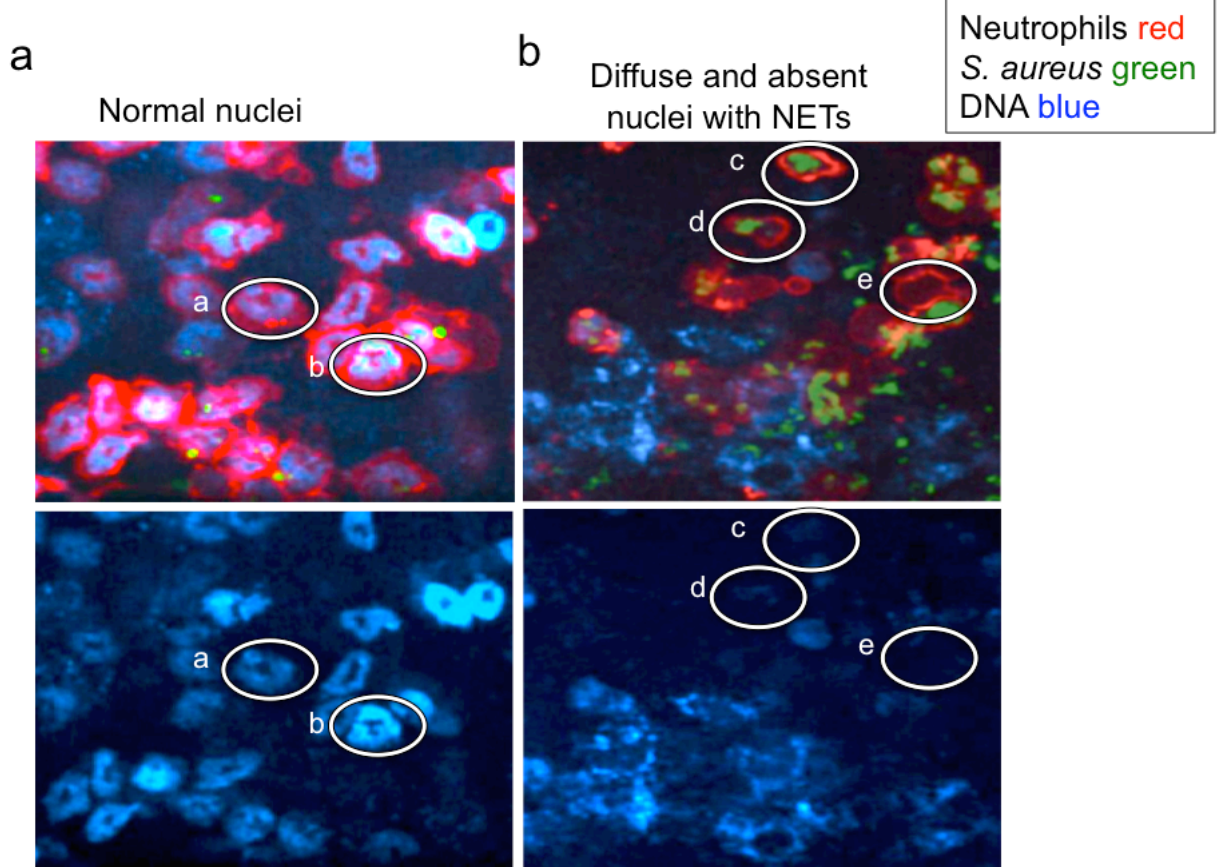
**Supplementary Figure 4.** *In vivo* neutrophil responses to live *S. aureus*. **(a)** Emigrated neutrophils were enumerated during each time interval. **(b)** Cell polarity was determined from manual measurements of long axis/short axis in each of the groups. (For comparison to sterile inflammation \* =  $P < 0.05$  and for comparison to wild type ### =  $P < 0.001$ ). **(c)** Dissemination was evaluated by quantifying bacteremia 5 h after a local injection of live *S. aureus* (Xen8.1,  $1 \times 10^8$  CFU in a 200  $\mu$ l saline injection) into the intraperitoneal cavity. Seventeen mice were used for these experiments (\* =  $P < 0.05$ ).

## Supplementary Figure 5



**Supplementary Figure 5.** Live *in vivo* PMN release extracellular DNA as NETs. PMN (PE-conjugated Ly6G specific antibody, red) were pre-labeled with a cell permeable nuclear dye (SYTO 60, blue). (a) Demonstrates the 3D cell surface of a normal and a NETTing PMN. (b) Demonstrates the cell surface with the addition of 2D DNA imaging. Note extracellular DNA is only visible in the NETTing PMN. (c) Altering the translucency of the PMN outer membrane demonstrates that the normal PMN has a normal and completely intracellular nucleus, while the NETTing PMN has both intracellular and extracellular DNA. (d) The velocities, (e) meandering index and (f) tracking is demonstrated for PMN visualized that are actively releasing NETs. Examples of NETTing PMN are shown in Supplementary Video 4.

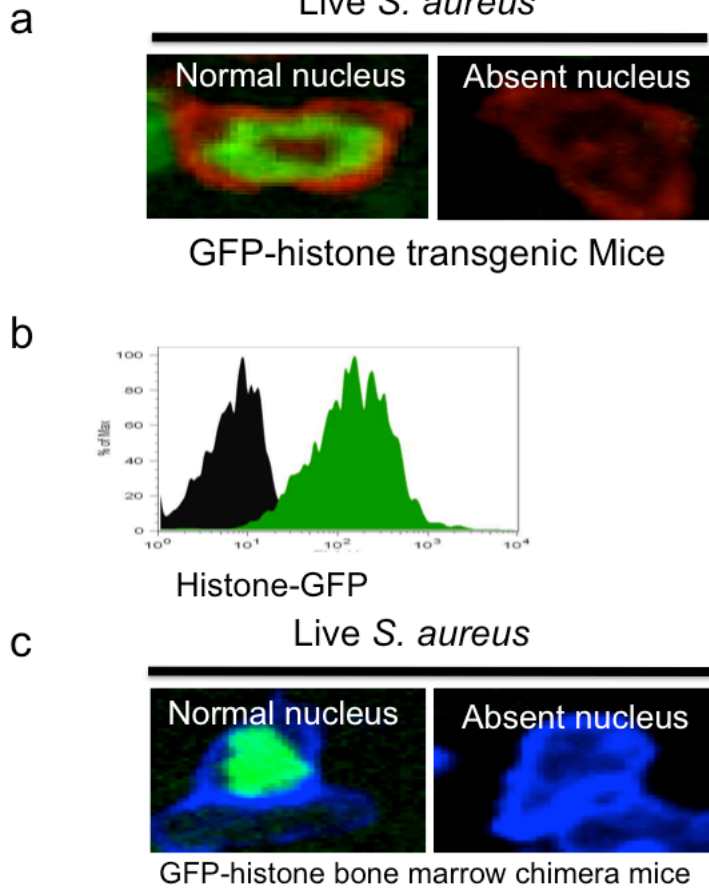
Supplementary Figure 6



**Supplementary Figure 6.** *In vivo* intracellular imaging of live PMN during infection. Spinning disk confocal intravital microscopy was performed on mice pre-treated with the cell-permeable nucleic acid dye (SYTO 60, blue) followed by chemokine (MIP-2, 0.2  $\mu\text{g}$  intradermal), GFP-*Staphylococcus aureus* (GFP-USA300,  $1 \times 10^8$  CFU in 100  $\mu\text{l}$  intradermal saline injection) and PE conjugated GR-1 specific antibody (i.v.). **(a)** Normal nuclear structure can be observed in PMN marked a and b. No extracellular DNA is observed adjacent to normal PMN. **(b)** PMN within an area of high bacterial burden. Cells marked c and d are anuclear and have taken up GFP-bacteria, while cell e is anuclear prior to phagocytosing bacteria. Substantial NETs (blue outside of PMN cellular membranes) can be observed in the high bacterial areas. The images are representative of 5 individual experiments with 5 mice.

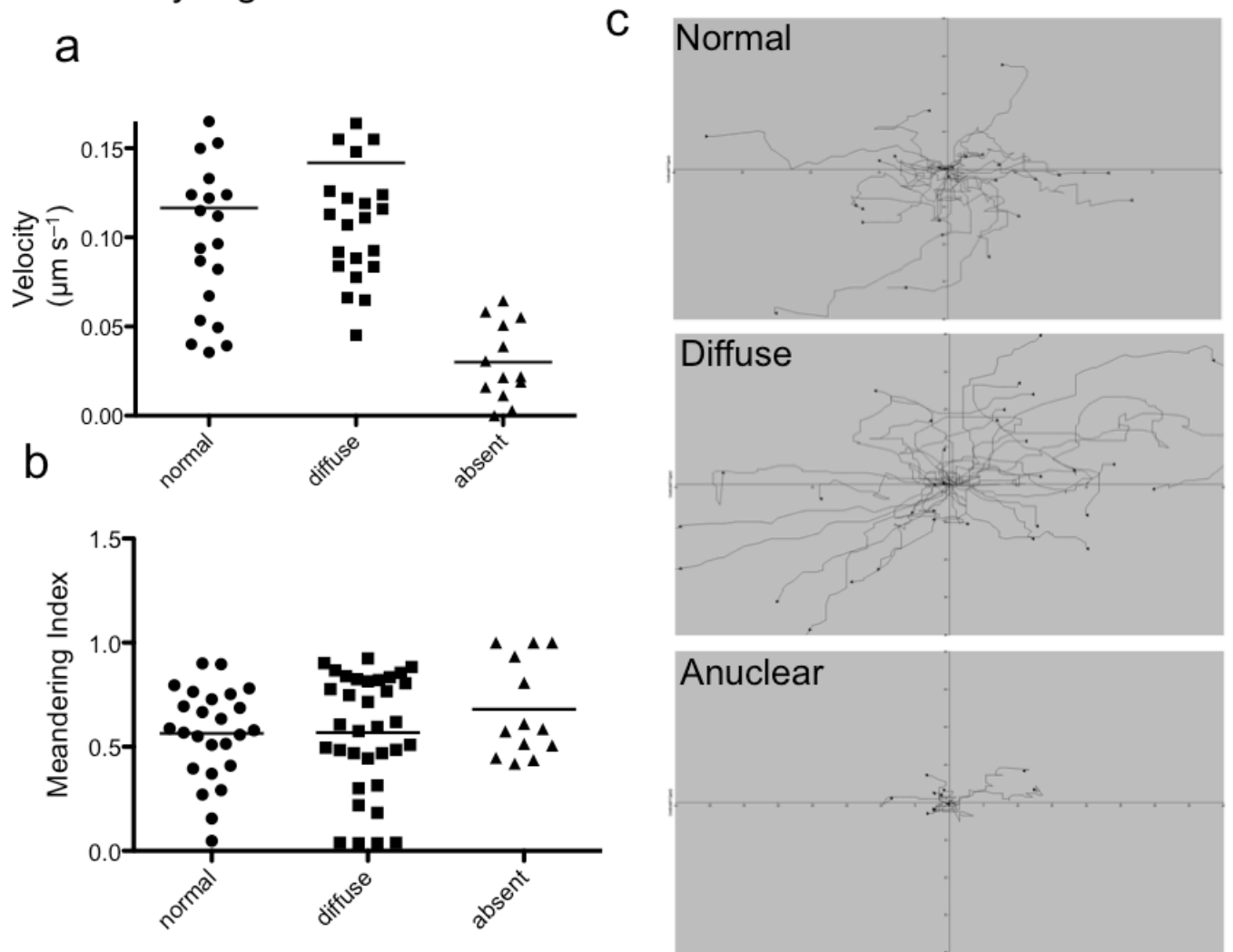


Supplementary Figure 7 Live *S. aureus*



**Supplementary Figure 7.** *In vivo* imaging of histone-GFP transgenic mice. (a) Spinning disk confocal intravital microscopy was used to visualize emigrated PMN of transgenic histone-GFP mice treated with live *S. aureus* (Xen8.1,  $1 \times 10^8$  CFU in 100  $\mu$ l saline injection). Left image shows a normal PMN nucleus while the right shows an anuclear PMN. Neutrophils were labeled with PE conjugated GR-1 specific antibody (Images represent 3 independent transgenic animal experiments with 3 mice). (b) The baseline GFP expression levels of unstimulated cells gated for GR-1<sup>+</sup> (PMN) is displayed from spleen transgenic-GFP animals (green population) versus unstimulated wild type animals (black population). Flow cytometry was repeated with 4 transgenic animals in 4 separate experiments. (c) Representative images from bone marrow chimeric animals that express histone-GFP only within hematogenous cells and have received live *S. aureus* (Images represent 4 bone marrow chimeric animals).

## Supplementary Figure 8



**Supplementary Figure 8.** *In vivo* tracking of live PMN with normal, diffuse and absent nuclei. We pre-treated mice with SYTO 60 to pre-label the nuclei (Method 3) and mice were treated with live *S. aureus* (GFP-USA300,  $1 \times 10^8$  CFU in 100  $\mu\text{l}$  intradermal saline injection). PMN that had normal, diffuse or absent nuclei were tracked. **(a)** Velocity and **(b)** meandering index or shown. **(c)** Individual tracks are displayed.

Supplementary Table 1

<u>Age</u>	<u>Past Medical History</u>	<u>Clinical Presentation</u>	<u>Microbiology</u>
72yr F	<ul style="list-style-type: none"> <li>•Hypertension</li> <li>•COPD</li> <li>•Arthritis</li> <li>•Smoker</li> <li>•Depression</li> </ul>	<ul style="list-style-type: none"> <li>•Right ankle cellulitis with secondary abscess formation</li> <li>•3 days duration prior to presentation</li> <li>•Empirically treated as gram-positive infection prior to culture</li> </ul>	Culture negative
38yr M	<ul style="list-style-type: none"> <li>•Healthy</li> </ul>	<ul style="list-style-type: none"> <li>•Right lower leg cellulitis with secondary abscess formation following an abrasion</li> <li>• 4 day duration prior to presentation</li> <li>•Treated for <i>Staphylococcus aureus</i></li> </ul>	Culture positive for community acquired antibiotic resistant <i>S. aureus</i> (MRSA)
26yr F	<ul style="list-style-type: none"> <li>•Depression</li> <li>•Remote intravenous drug abuse</li> </ul>	<ul style="list-style-type: none"> <li>•Left foot abscess formation following laceration</li> <li>•2 weeks duration prior to presentation</li> </ul>	Culture positive for antibiotic sensitive <i>S. aureus</i> (MSSA)
51yr M	<ul style="list-style-type: none"> <li>•Gastroesophageal reflux disease</li> </ul>	<ul style="list-style-type: none"> <li>•Right knee post-operative incision infection and secondary abscess</li> <li>•Presented 1wk post-operative</li> <li>•Treated empirically as gram-positive (presumed <i>S. aureus</i>) wound infection and abscess</li> </ul>	Culture negative
70yr M	<ul style="list-style-type: none"> <li>•Type 2 Diabetes</li> <li>•Hypertension</li> <li>•Chronic kidney disease</li> </ul>	<ul style="list-style-type: none"> <li>•Left lower arm arterial-venous (A-V) fistula infection with abscess formation</li> <li>• 3 day duration prior to presentation</li> <li>• 2weeks from A-V fistula surgery</li> </ul>	Culture positive for antibiotic sensitive <i>S. aureus</i> (MSSA)

Supplementary Table 1. Human patient histories and microbiology.

